

Supplemental Data Set 1

FPKM expression for immune checkpoint genes and FOXP3 for matched peripheral and tumor Treg RNA seq samples for patients from four cancer types.

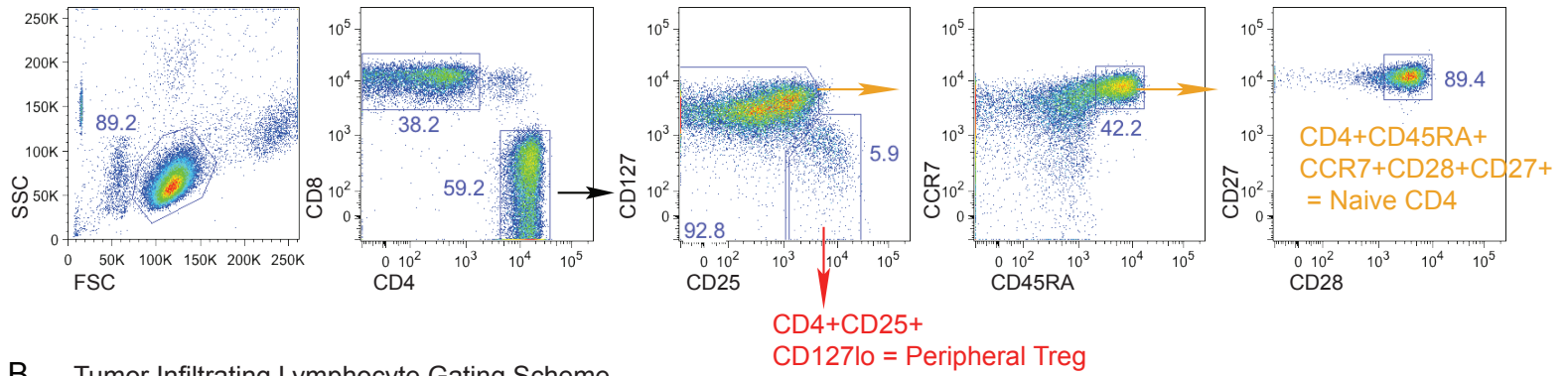
Supplemental Figure Legends

Figure S1 Sorting strategy for purifying CD4 T cell subsets.

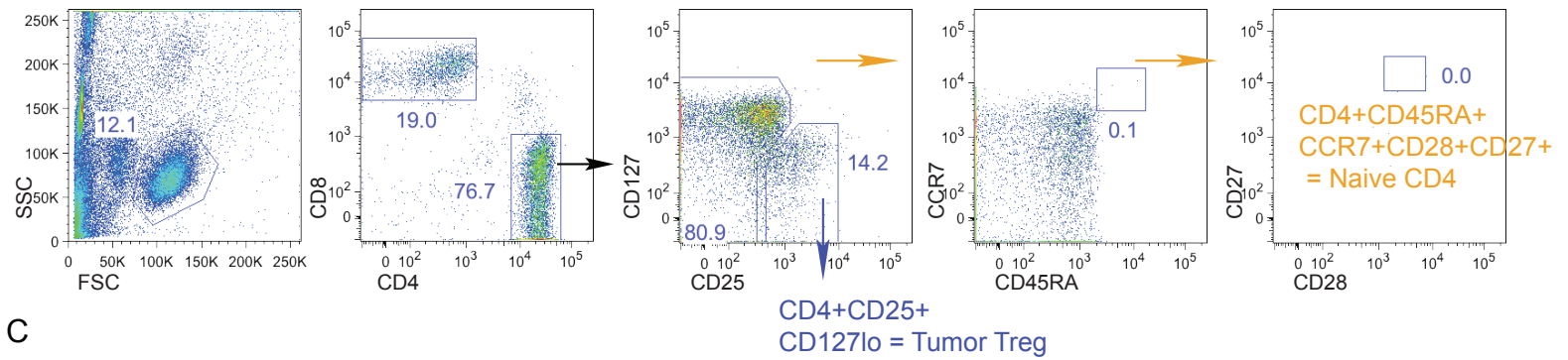
Representative sample of flow cytometry for individual patient samples that underwent FACS sorting purification for T cell subsets. A) Gating strategy for peripheral blood naïve CD4⁺CD45RA⁺CCR7⁺CD28⁺CD27⁺ T cell and CD4⁺CD25⁺CD127^{Low} Treg subsets (Peripheral Tregs). B) Gating strategy for tumor origin CD4⁺CD25⁺CD127^{Low} Treg subset (Tumor Tregs). Post sort purity for Naïve CD4⁺ T cells (C), peripheral Tregs (D), and tumor derived Tregs (E).

Figure S1

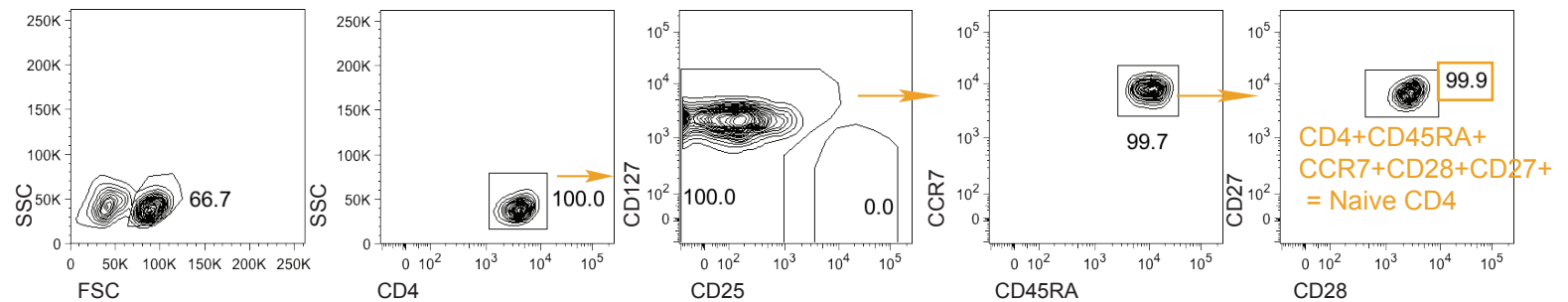
A Peripheral Blood Lymphocyte Gating Scheme



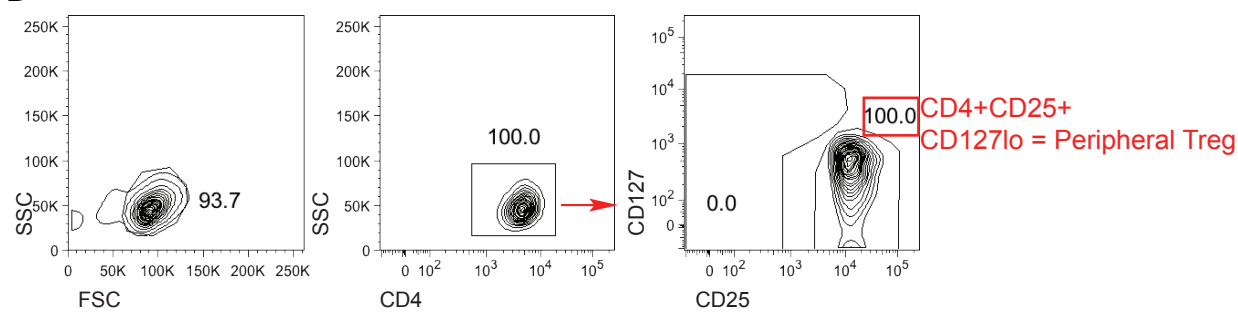
B Tumor Infiltrating Lymphocyte Gating Scheme



C Peripheral Naive CD4 Post Sort Purity



D Peripheral Treg Post Sort Purity



E Tumor Treg Post Sort Purity

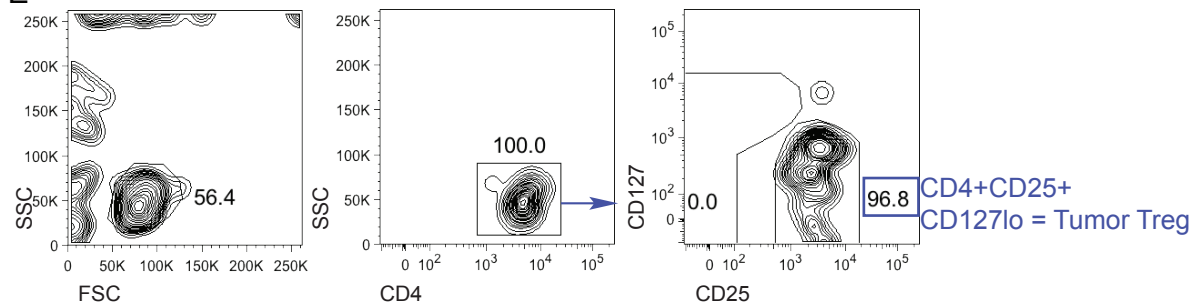
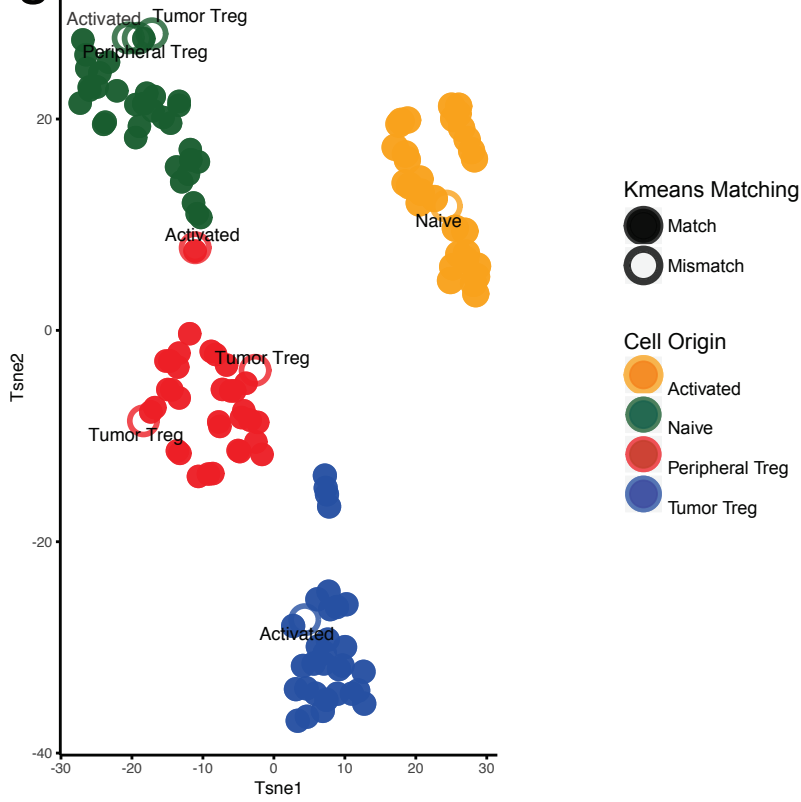


Figure S2. Immune checkpoint molecule expression identifies CD4 T cell subsets across cancers.

A) Clustering analysis for immune checkpoint gene expression in purified CD4 T cell subsets for irrespective of cancer type. Kmeans clustering was used to assign labels based on clustering groups and then original labels were assigned to check identification. Open circles represent mismatches in the Kmeans clustering assignment to the true cell identity. B) Expression of checkpoint molecules in purified naïve (green) and activated (orange) CD4 T cells across all four cancer types. Top annotation row designates CD4 T cell origin and second annotation row identifies patient tumor type.

Figure S2

A



B

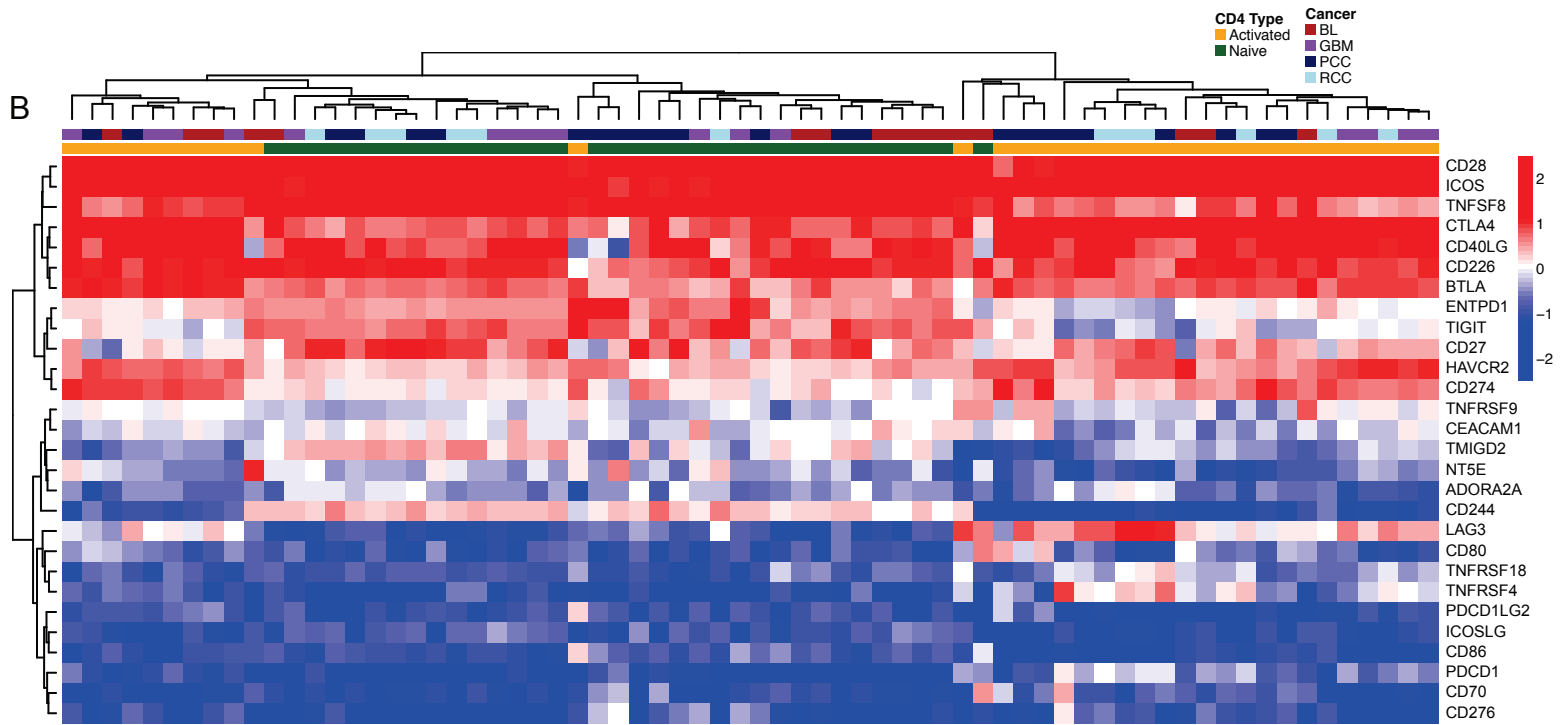
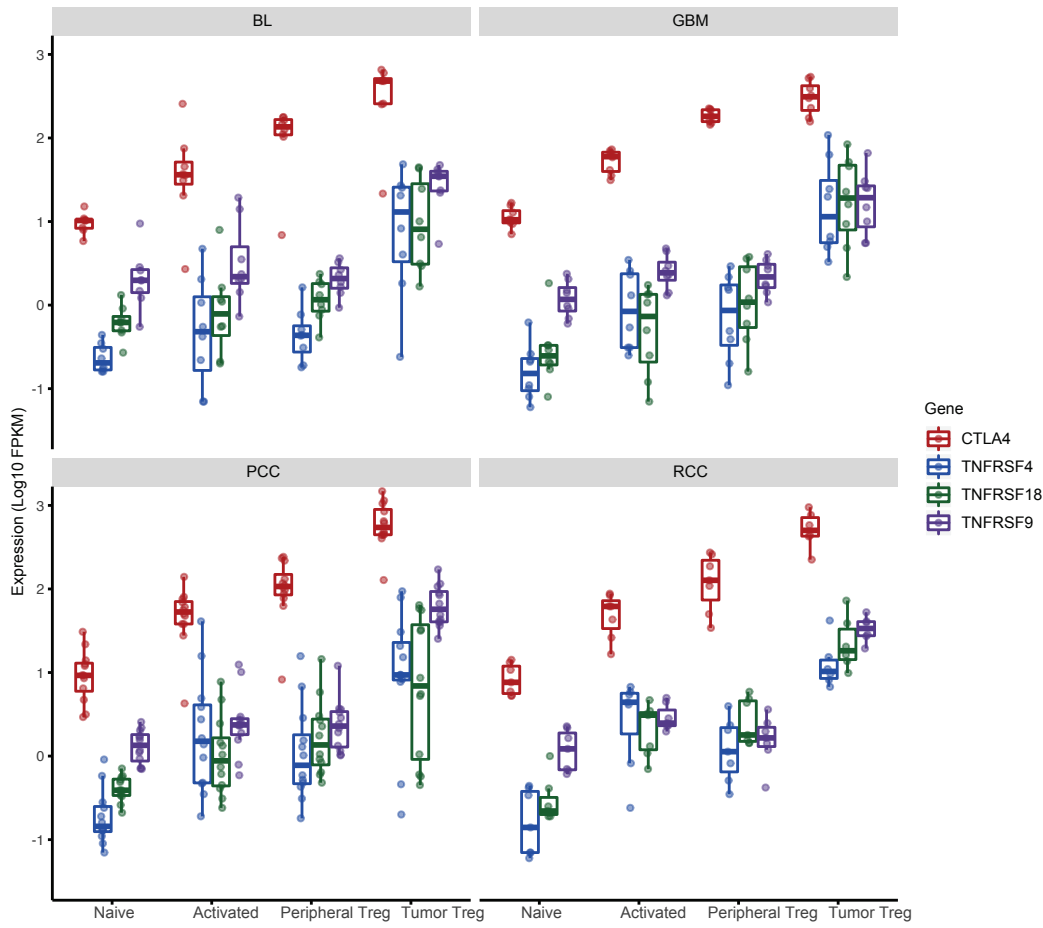


Figure S3. Tumor Tregs express distinct checkpoint molecules compared to other CD4 T cell types.

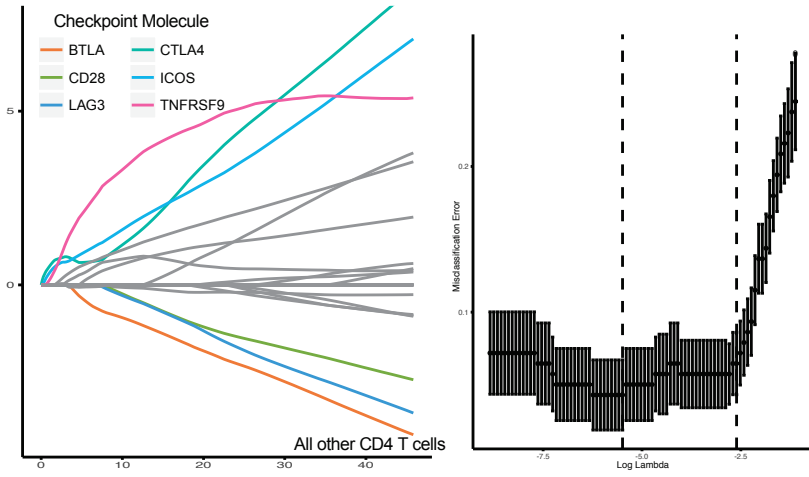
A) Expression across all CD4 subsets in each cancer type CTLA-4 and TNFR family members. Across 4 cancer types. B) Spaghetti plot of logistic regression with LASSO normalization comparing checkpoint molecule expression in tumor Tregs compared to other CD4 T cell subsets. Highlighted lines represent top 3 checkpoint molecules that discriminate tumor Tregs (TNFRSF9, CTLA-4, ICOS) and other CD4 T cell subsets (BTLA, CD28, LAG3) from each other. Leave one out cross validated logistic regression with LASSO normalization to determine ideal lambda min for coefficient selection to identify checkpoint genes for most cell subsets. C) Spaghetti plot of logistic regression with LASSO normalization comparing checkpoint molecule expression in tumor Tregs compared to peripheral Tregs. Highlighted lines represent top 3 checkpoint molecules that discriminate tumor Tregs (TNFRSF9, HAVCR2, LAG3) and other peripheral Tregs (CD28, ENTPD1, TMIGD2) from each other. Leave one out cross validated logistic regression with LASSO normalization to determine ideal lambda min for coefficient selection to identify checkpoint genes for most cell subsets.

Figure S3

A



B



C

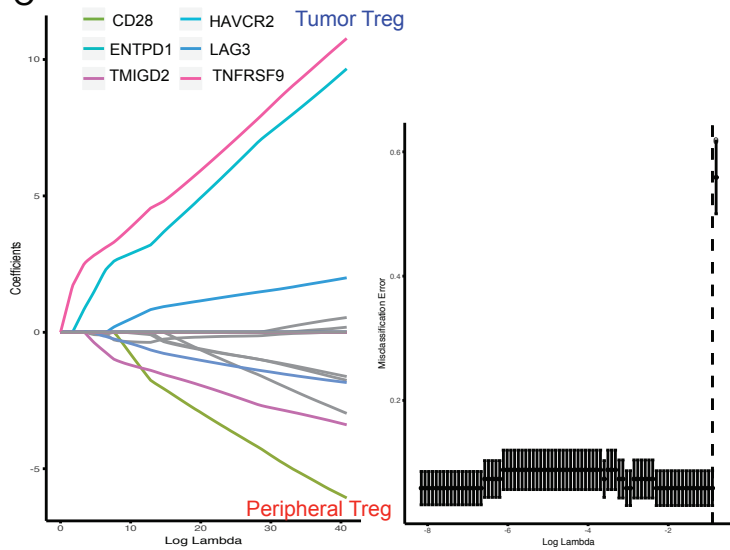
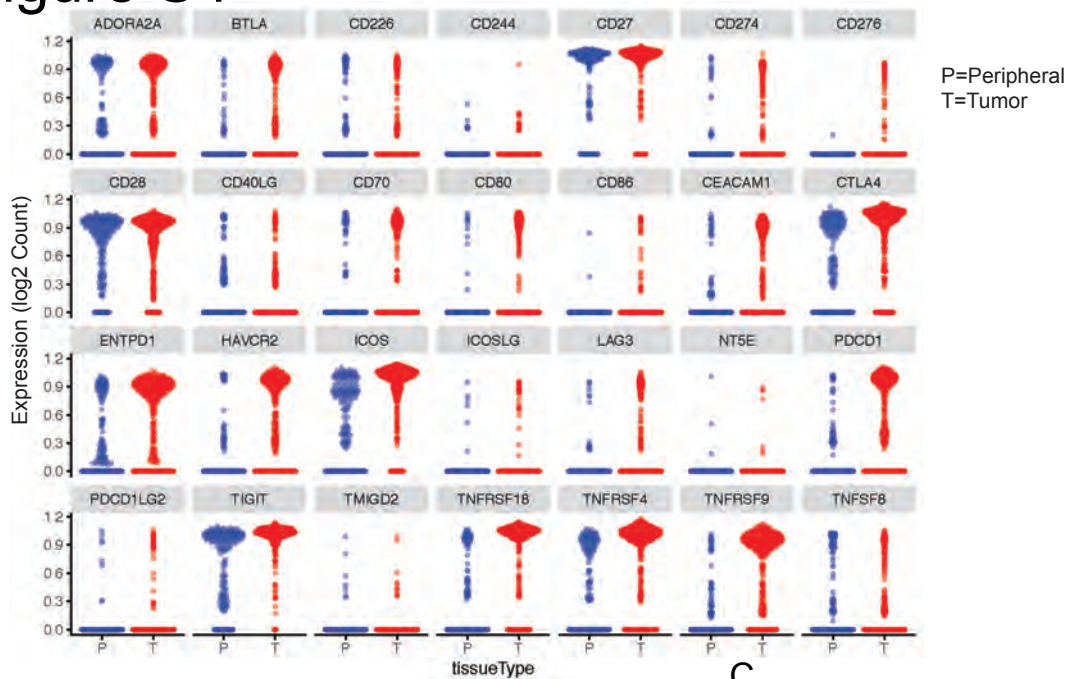


Figure S4. 4-1BB expression is preferentially upregulated on single cell Tregs from liver hepatocellular carcinoma.

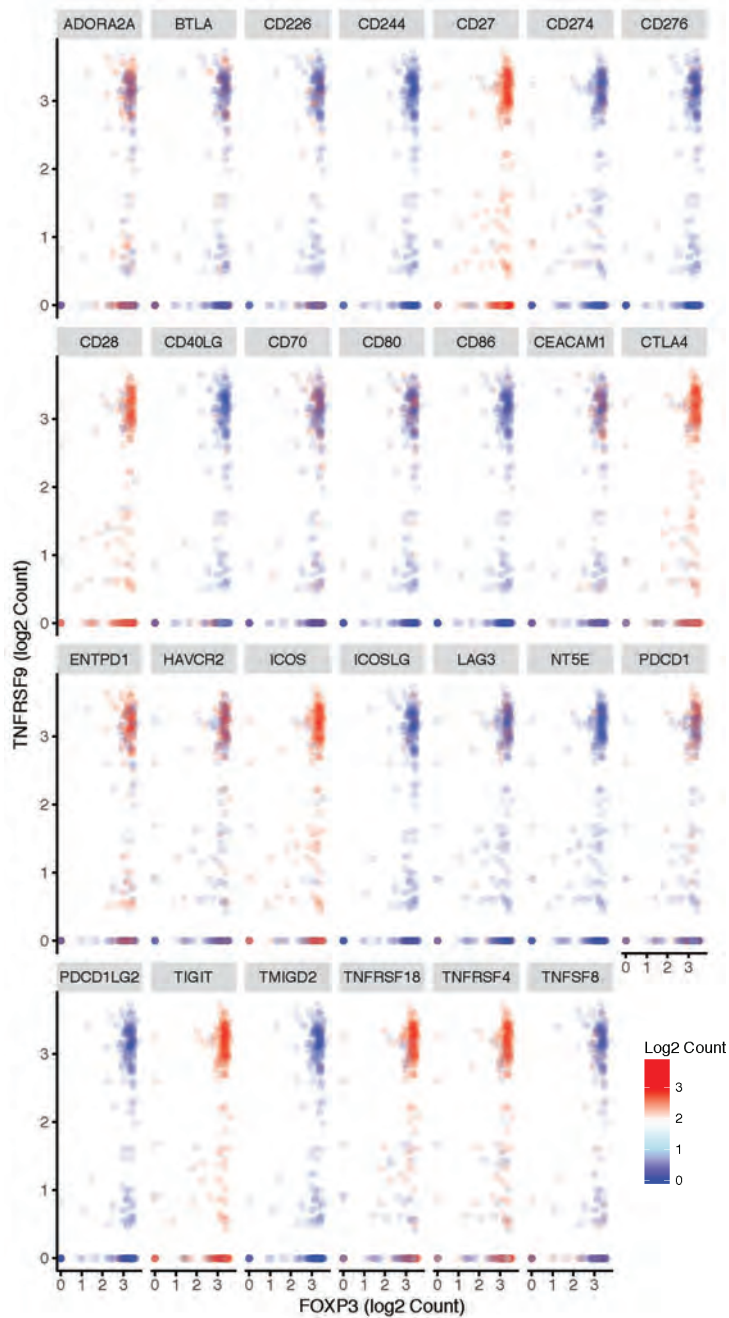
A) Single peripheral (P) and tumor (T) Treg expression of immune checkpoint genes in cells enriched from three patients with liver cancer(28622514). B) Co-expression of FOXP3 and TNFRSF9 in tumor origin Tregs. Color represents expression of checkpoint molecule labeling each tile across the individual cells. C) 4-1BB RNA levels in purified tumor Tregs and CD8 T cells across 4 different cancers (BL = bladder cancer, GBM = glioblastoma, PCC = prostate cancer, RCC= renal clear cell cancer). D) Flow cytometry of T cells isolated from various cancers for 4-1BB protein expression. Log₁₀ 4-1BB MFI for CD4+FOXP3⁻, CD4+FOXP3⁺ (Treg) and CD8 T cell subsets. 4-1BB MFI are plotted across paired samples for CD4+FOXP3⁺ (Treg) and CD8 T cell subsets. Friedman test with Dunn's posttest or paired *t*-test were used to compare groups. (n=6 total patients, 4 cancer types) ($P < 0.05$ *, $P < 0.01$ **)

Figure S4

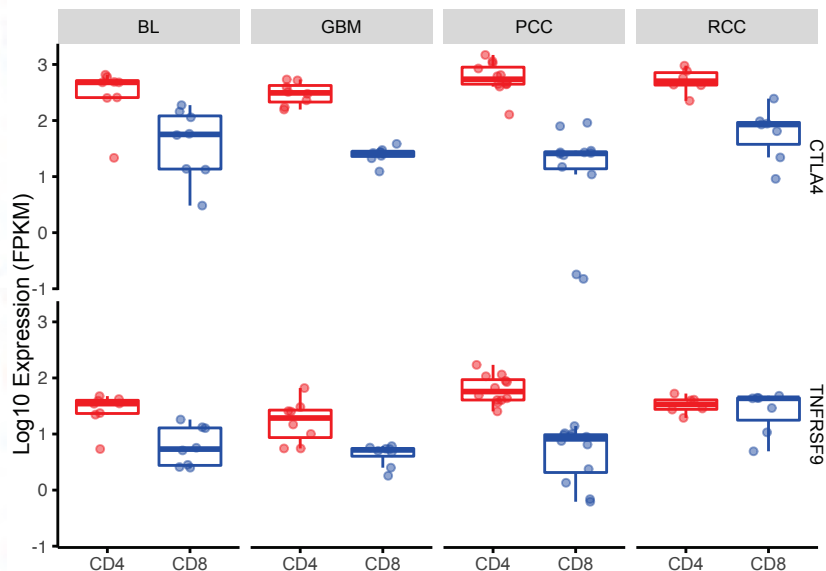
A



B



C



D

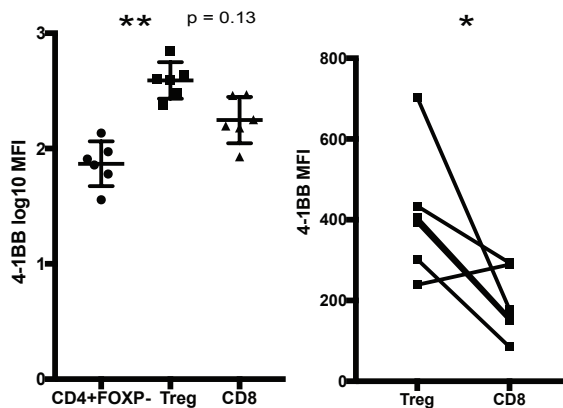


Figure S5. Normal tissue and cancer have distinct Treg FOXP3 associated checkpoint molecule expression.

A) Normalized tissue and cancer expression overlaid onto tissue immune checkpoint clustering tSNE analysis for Treg correlated immune checkpoints. B) Expression ($\log_{10} \text{RSEM}+1$) of Treg correlated immune checkpoints across multiple normal and cancer tissue matched samples demonstrating the normal and cancer landscape.

Figure S5

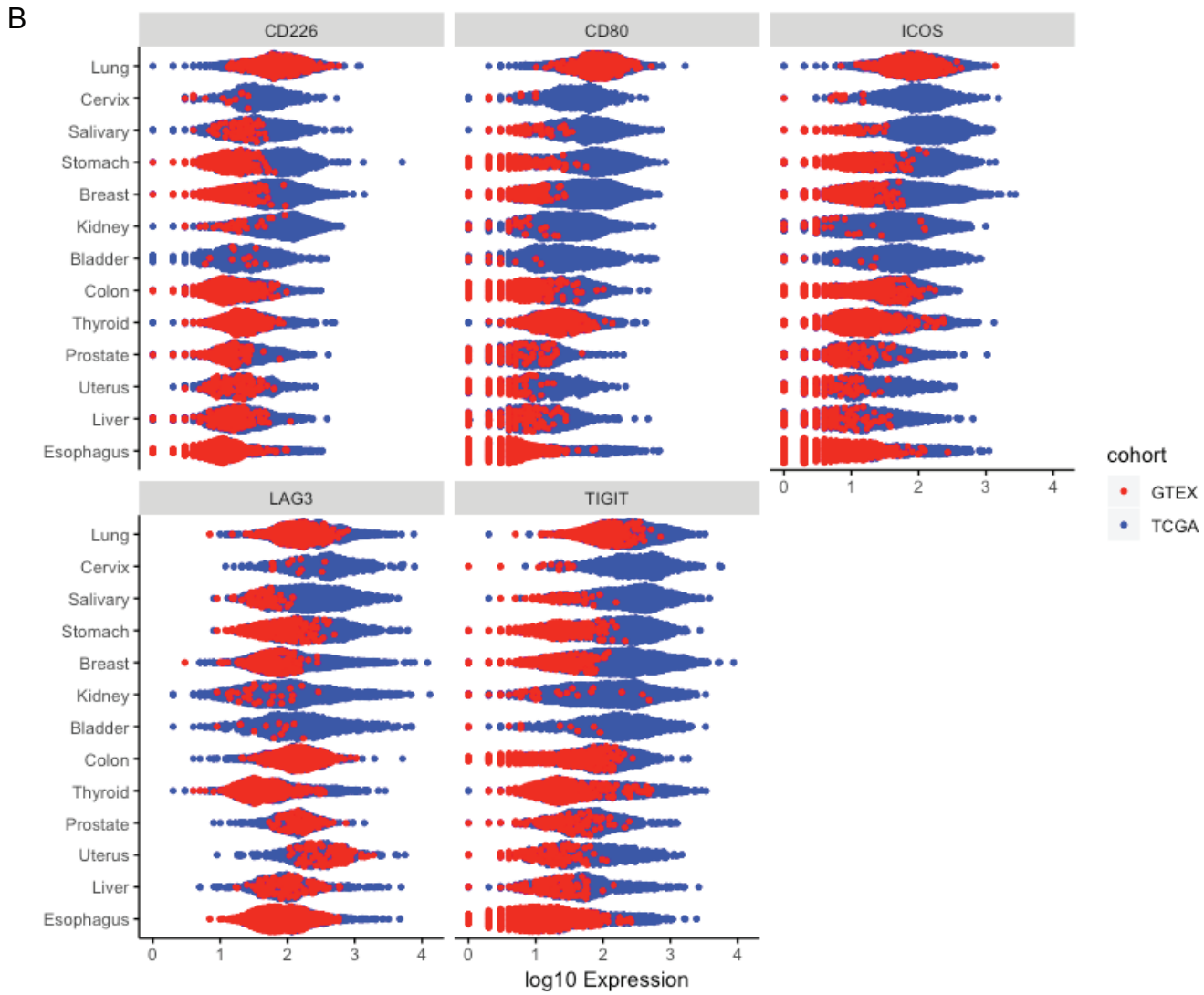
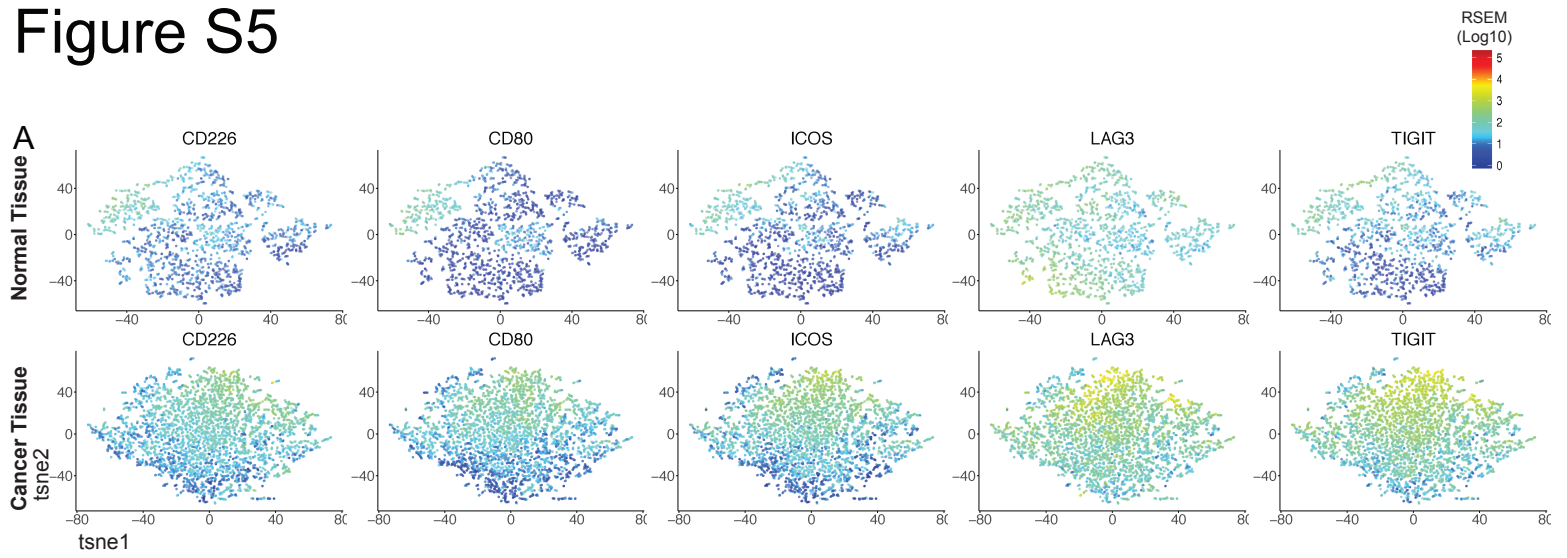


Figure S6. 4-1BB targeting by IgG2a and IgG1 antibody isotypes decrease tumor growth by differentially affecting Tregs and CD8 T cells.

A) Tumor growth curves for individual mice with MC38 tumors treated with Isotype control, anti- 4-1BB (IgG2a), anti- 4-1BB (IgG1), or anti- PD-1. B) Summary or median tumor growth curves for mice treated as in A. C) Survival curves for mice treated as in A. D) Tumor infiltrating lymphocyte frequencies for CD8+, CD4+, and FOXP3+ T cells from mice treated with Isotype control, anti 4-1BB (IgG2a), anti 4-1BB (IgG1), or anti- PD-1. E) Spleen lymphocyte frequencies for CD8+, CD4+, and FOXP3+ T cells from mice treated with Isotype control, anti 4-1BB (IgG2a), anti 4-1BB (IgG1), or anti- PD-1. F) G) Granzyme B and PD-L1 expression on tumor Tregs from mice with Isotype control, anti- PD-1, anti 4-1BB (IgG1), or anti 4-1BB (IgG2a) antibodies. H) Granzyme B and PD-L1 expression on tumor CD8 T cells from mice with Isotype control, anti- PD-1, anti 4-1BB (IgG1), or anti 4-1BB (IgG2a) antibodies. Representative example of 2 experiments. (n=12 for survival studies, n = 4-5 for flow cytometry studies)

Statistical comparisons were performed using repeated measures ANOVA with Tukey multiple comparisons test for tumor growth curves response to treatment and one-way ANOVA with Dunnet multiple comparisons test for intra tumor analysis of different T cell populations. ($P < 0.01$ **, < 0.001 ***, < 0.0001 *****)

Figure S6

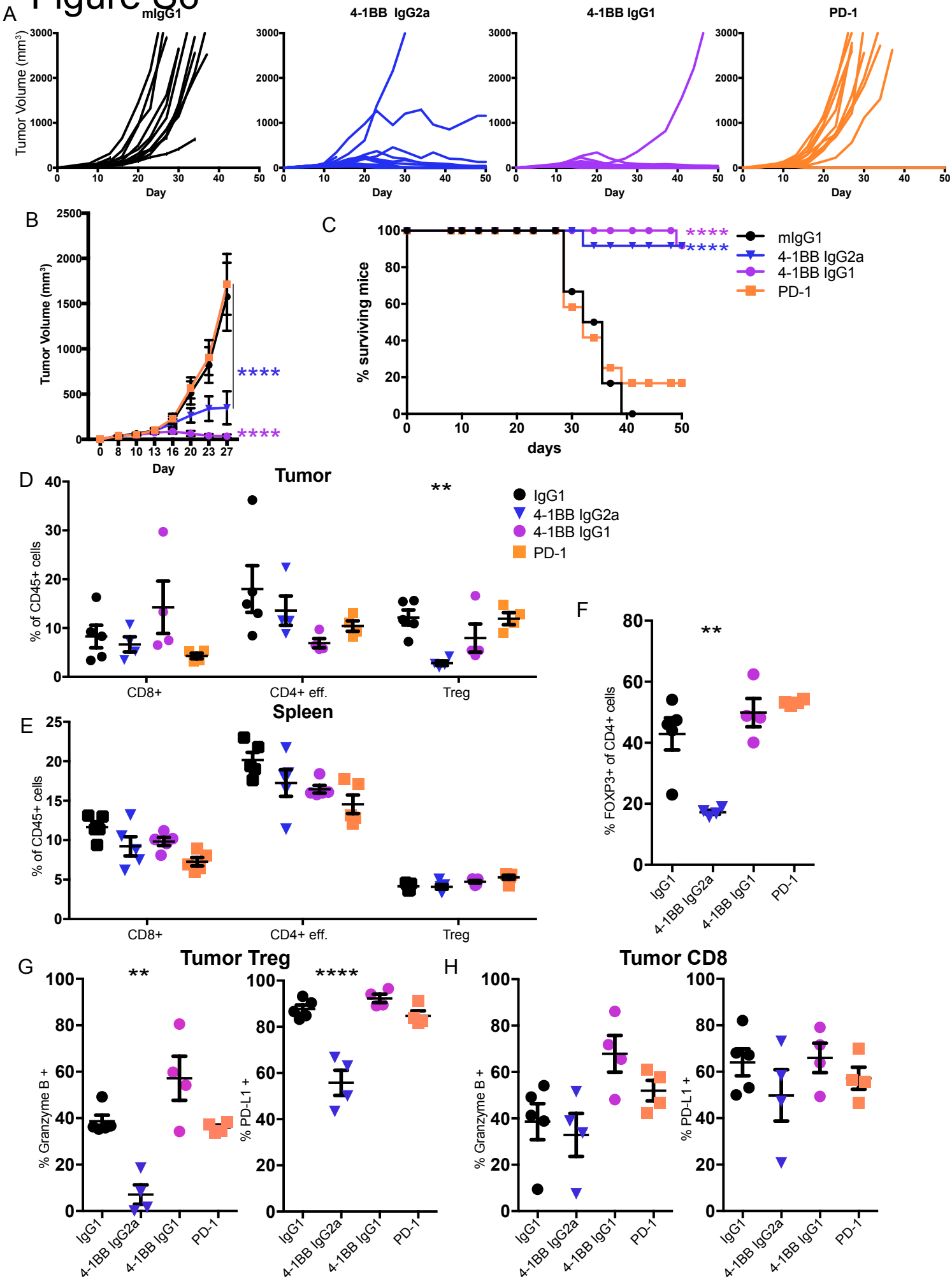


Figure S7. CD8 GZMK expression associated with differential survival across cancers.

A) Kaplan Meier curve for survival based on CTLA4/FOXP3, TNFRSF4/FOXP3, and TNFRSF18/FOXP3 ratio for thirteen cancers from TCGA. B) Kaplan Meier curve for survival based on CD8A or FOXP3. C) Expression (log₁₀) of CD8A and GZMK across cancers identifying CD8A GZMK high and low cohorts. D) Kaplan Meier curve for survival based on quantiles of CD8A and GZMK expression. E) Expression (log₁₀) of CD8A and GZMK across thirteen cancers identifying CD8A GZMK high and low cohorts.

Figure S7

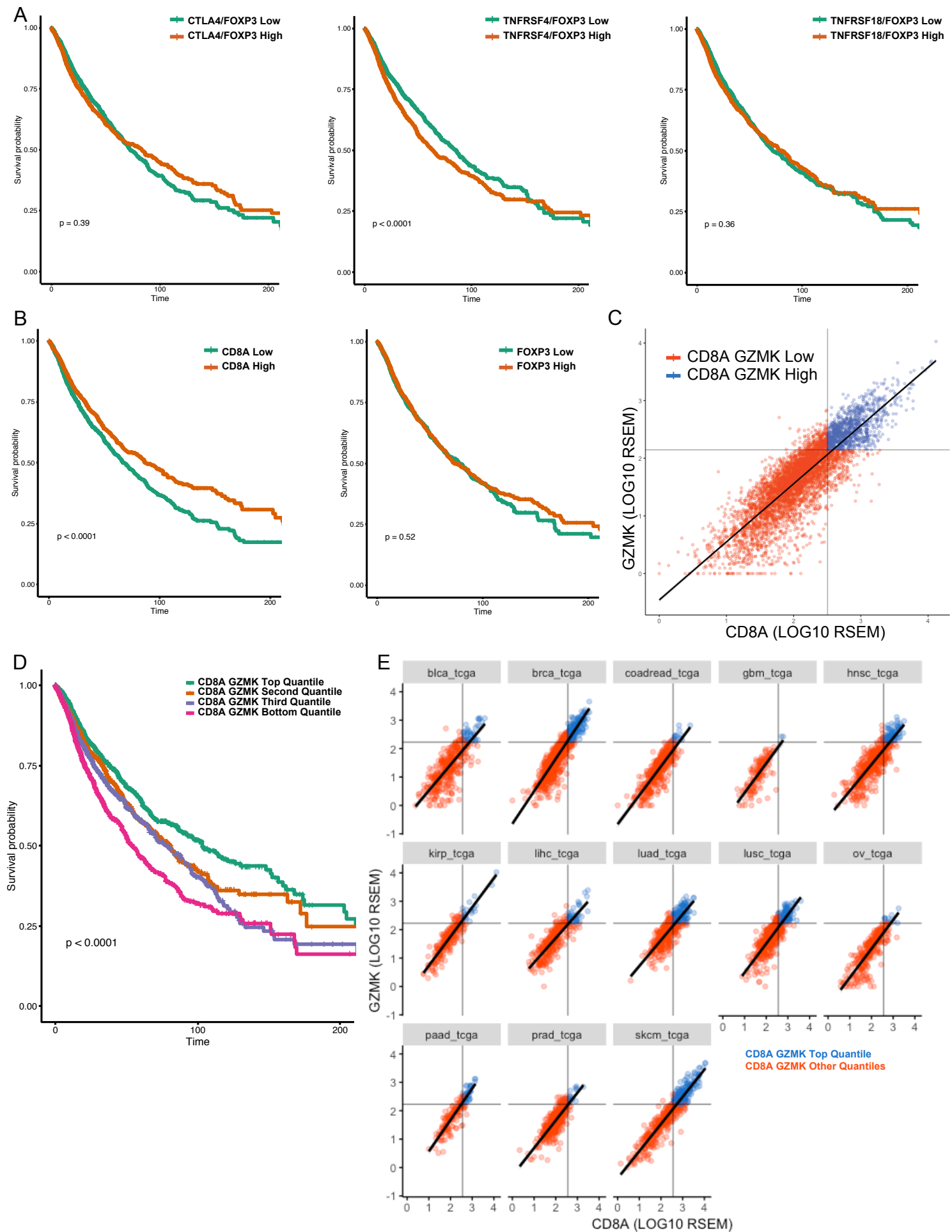


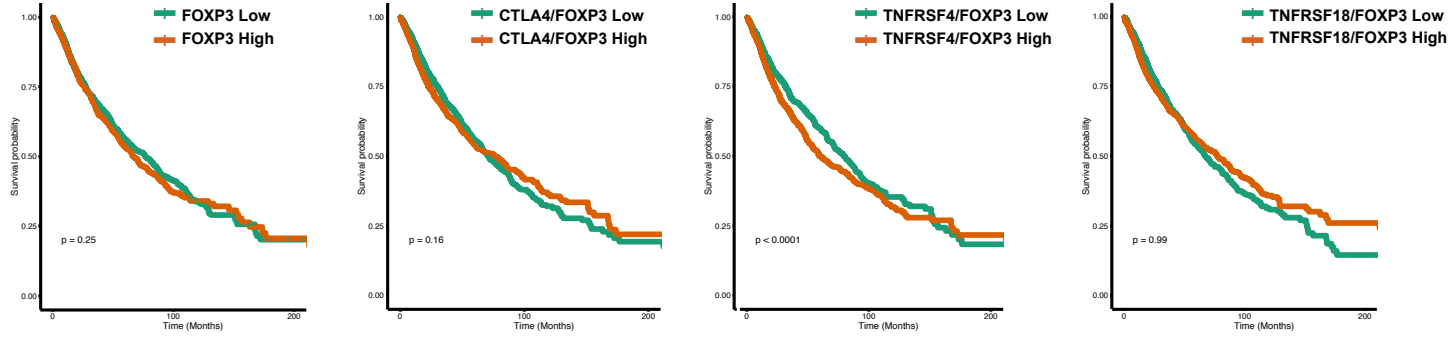
Figure S8. Treg immune checkpoint expression in CD8 GZMK high and low cancers.

A) Kaplan Meier curves for FOXP3, CTLA4/FOXP3, TNFRSF4/FOXP3, and TNFRSF18/FOXP3 in the CD8 GZMK low cohort. B) Kaplan Meier curves for FOXP3, CTLA4/FOXP3, TNFRSF4/FOXP3, and TNFRSF18/FOXP3 in the CD8 GZMK high cohort. C) Correlation of 4-1BB/FOXP3 with CD8A, GZMK, and perforin 1 (PRF1) levels in CD8 GZMK high and low cohorts.

Figure S8

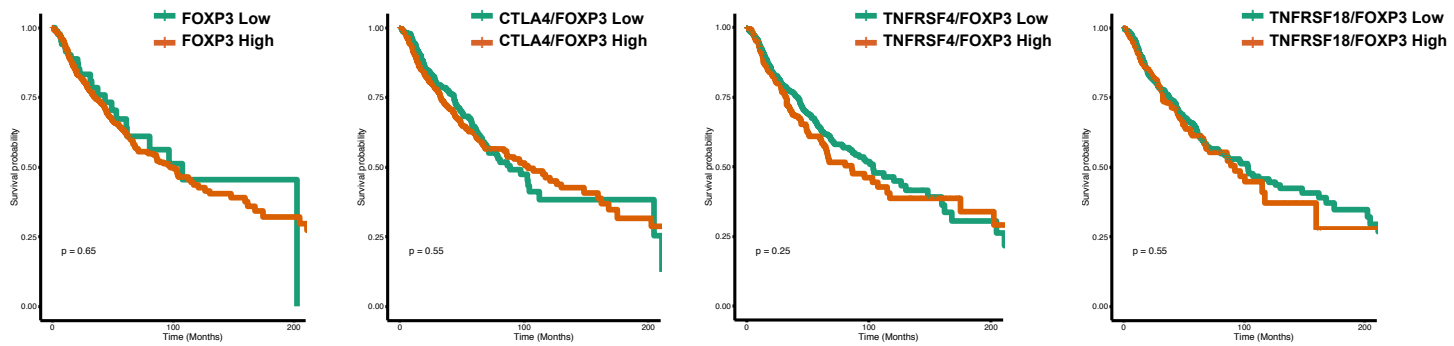
A

CD8 Low

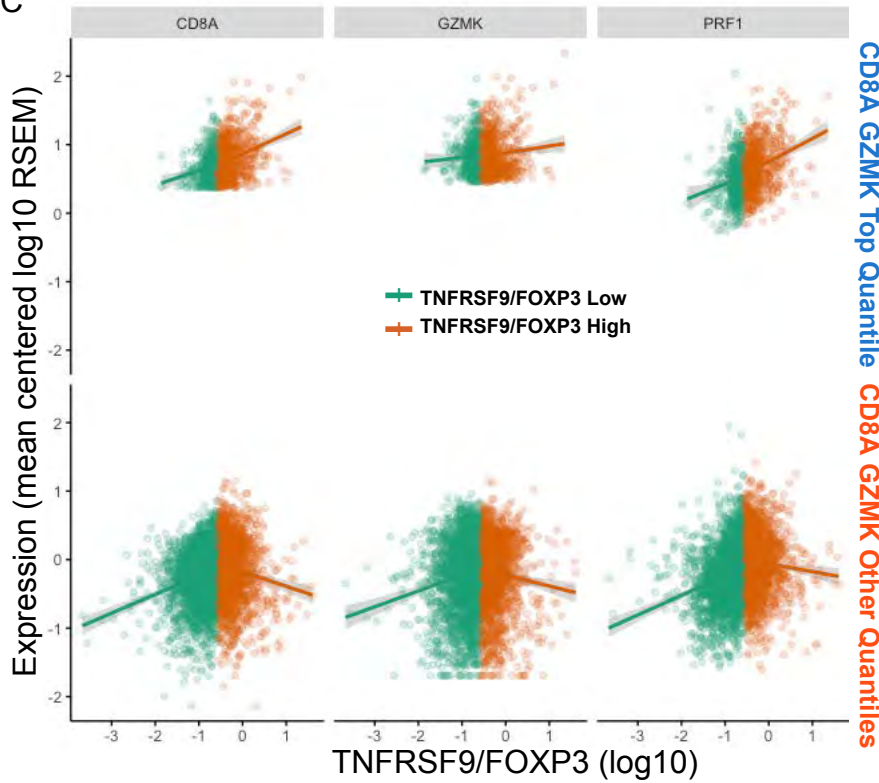


B

CD8 High



C



CD8A GZMK Top Quantile
CD8A GZMK Other Quantiles

Figure S9. Loss of 4-1BB in Tregs impairs suppressive function.

Murine Tregs were isolated using FACS sorting and in vitro Treg suppression assays performed to examine 4-1BB associated function in Tregs. A) Responder cell proliferation for Treg suppression assay with CD4 or CD8 T cells as responder cells. Cultures were treated with either isotype or non-depleting IgG1 antibody targeting 4-1BB for the duration of the experiment. B) Representative CFSE plots at varying Treg to responder cell ratios for TNFRSF9 fl/fl and FOXP3Cre⁺ TNFRSF9 fl/fl Tregs (representative example from 3 independent experiments). C) Responder cell proliferation for TNFRSF9 fl/fl and FOXP3Cre⁺ TNFRSF9 fl/fl Tregs at varying responder Treg to responder ratios. D-F) Flow cytometry for 4-1BB (D), CTLA-4 (E), and PD-1 (F) on the surface of TNFRSF9 fl/fl and FOXP3Cre⁺ TNFRSF9 fl/fl Tregs at cessation of Treg suppression assay.

Figure S9

